Vol. 329: 157–168, 2007 | MARINE ECOLOGY PROGRESS SERIES
Mar Ecol Prog Ser | Published January 11

Non-destructive measurement of the time evolution of burrowing shrimp mound topography

N. J. Grigg*, I. T. Webster, P. W. Ford

CSIRO Land & Water, Black Mountain Laboratories, GPO Box 1666, Canberra ACT 2601, Australia

ABSTRACT: We applied a profiling laser scanner system, originally developed for quantitative soil erosion studies, to produce 3-dimensional maps of underwater mounds produced in aquaria by thalassinidean shrimp *Trypaea australiensis*. With appropriate calibration against a surface of known geometry installed within the aquaria, the technique is highly accurate (1 and 2 mm resolution in the 2 horizontal dimensions and 0.2 mm resolution in the vertical). The method is non-destructive, and the evolution of mounds can be measured so the net daily rate of movement of material from the burrow to the surface mound can be reliably estimated. The technique also detects and measures slumping of the mound material to produce 'funnels' — a process which cannot be characterised by conventional techniques based on direct entrapment of sediment. We used the technique to measure mound and funnel formation in 3 laboratory aquaria populated with thalassinidean shrimp over a period of 359 d. Significant changes in mound volume were observed to occur from one day to the next (mean rates of sediment rise ranged from 0.36 to 1.1 $cm^3\ d^{-1}$ $opening^{-1}$, and mean rates of sediment fall ranged from –0.32 to –1.3 $cm^3\ d^{-1}$ $opening^{-1}$). The rapid rate of movement of material, both into and out of the burrow, has important implications for sampling frequency if the rates of movement of sediment are not to be drastically underestimated. Our results suggest that daily sampling is required. This is rarely achieved in other studies, and, consequently, existing published values may be too low. The technique could be applied to quantify sediment transfer by other species that produce perturbations in the level of the sediment surface.

KEY WORDS: Thalassinidean shrimp · Sediment turnover · Bioturbation · Mound

INTRODUCTION

Thalassinidean shrimp (Crustacea: Decapoda) exist in marine and brackish water bodies all around the world (excluding Arctic and Antarctic regions). Approximately 516 species have been described so far; 95% of these occur in water shallower than 200 m, and they burrow in sediments ranging from coarse coral rubble to sand and mud (Dworschak 2000). The burrow construction and irrigation activities of these shrimp have a significant influence on sediment biogeochemistry and fluxes between sediments and overlying water (Forster & Graf 1995, Ziebis et al. 1996, Bird et al. 1999, Webb & Eyre 2004). The most common species along the eastern Australian coastline is *Trypaea australiensis*, the subject of our experiments. For this particular species it is common to find burrows extending deeper than 1 m below the sediment surface (Webb & Eyre 2004), and the surface of sediments populated by these animals can have up to 300 openings m^{-2} (McPhee & Skilleter 2002).

Biogeochemical reactions in sediments are fuelled by the supply of organic matter. An active population of burrowing animals will ensure that organic matter is not simply a thin surface layer, accumulated through sedimentation from the water column. Rather, material may be translocated to considerable depths, or buried rapidly due to the expulsion of sediment from depth. The nature of thalassinidean shrimp burrowing points to both possibilities: sediment expulsion rates from their mounds are considerable, so creating high burial rates over the benthic surface surrounding the mound,

*Email: nicky.grigg@csiro.au

and their deep, permanent burrow structures trap organic matter drawn in by bioirrigation currents or mound collapse. Where shrimp burrowing is extensive, the cycling of particulate organic material associated with burrow building and collapse will have a profound effect on sediment diagenic processes and rates.

Given the important role of burrowing activities in aquatic biogeochemical processes, methods are needed to observe and quantify burrowing behaviour. Typically, measurements of animal mixing are described as a sediment turnover rate, for which there are a number of estimation methods. Rowden & Jones (1993) identified the 3 most common methods for measuring sediment turnover in thalassinidean shrimp populations, and discussed the relative advantages and disadvantages of each:

(1) Direct entrapment. A sediment trap positioned over a burrow opening collects ejected material. Rates are expressed as mass (wet or dry) or volume per mound, individual, or area per unit time. This is the most commonly used method.

(2) Levelling. An area of mounds is levelled and left for a known period of time. Any new material deposited on the surface is collected or the mound geometry is measured. Rates are expressed as mass or volume per unit area per unit time.

(3) Tracer particles. Labelled sediment (e.g. fluorescent dye or paint) is placed at known depth(s) in the sediment. Cores are taken after a known time, and the depth distribution of labelled particles is measured. Rates are expressed as a deposition depth per unit time.

Rowden & Jones (1993) concluded that these methods are not directly comparable, and can yield vastly different sediment turnover estimates for the same species. Their recommendations were to use the direct entrapment method, quote rates in terms of dry mass (rather than wet mass or volume), and to use the characteristics of the measurement to constrain the space and time units (e.g. if experiments were conducted over 1 wk, do not extrapolate to yearly estimates). Stamhuis et al. (1997) used a fourth method, which tracked the development of burrows by recording burrow outlines in thin cuvettes containing burrowing shrimp.

Drawbacks exist with the 3 methods described by Rowden & Jones (1993). Most importantly, they are all destructive methods in some way. The direct entrapment method removes ejected material and the levelling method has an unknown effect on sediment ejection rates. The tracer particle method needs a sectioned core to obtain just 1 estimate of turnover rates, so turnover rates as a function of time in 1 place are not possible and this method is most appropriate over long time scales. A significant advantage of the tracer particle method is that it can measure vertical transport within the sediment column, although the 1-shot nature of the measurements preclude tracking particles that may make multiple journeys to the surface and back. The burrow tracking method described by Stamhuis et al. (1997) is non-destructive and has the potential to track upward and downward transport of material, but requires manipulated laboratory conditions.

The present study made estimates of *Trypaea australiensis* sediment turnover rates in the laboratory using a laser scanner. The primary aim of the study was to investigate the usefulness of high spatial and temporal resolution measurements of burrow mounds; estimating *T. australiensis* turnover rates was a secondary aim, chiefly due to the artificial laboratory conditions. The laser scanner data allowed the creation of high resolution maps of the sediment surface, and the changes in mound topography over time were used to estimate rates of volume change. This technique has the advantage of being non-destructive, and it is able to detect both upward and downward transport at the sediment surface.

MATERIALS AND METHODS

Experimental set-up. The laser scanner design was based on the description in Huang et al. (1988), with the main modification from their description being the use of a 2-dimensional traversing frame rather than a 1-dimensional frame. The high-precision traversing frame was driven by stepper motors. The equipment consisted of a low-power helium-neon laser (633 nm, 10 MW), a 35 mm format single lens reflex (SLR) camera with a 50 mm lens, a 256 element linear photodiode array, a high-precision 2-dimensional traversing frame and associated electronics and software. The laser was mounted on the traversing frame and directed vertically downwards onto the sediment, creating a light point on the surface. The camera was mounted at a small angle to the laser, and the image of the laser point was focussed onto the photodiode array, which was fitted to the back of the camera (Fig. 1).

The position of the image on the diode array changes if the sediment surface height changes, and so can be used to determine sediment surface elevation. The shape of the image on the diode array could be observed using a cathode ray oscilloscope (CRO). The image was generally a bell-shaped curve spread across several diodes; its width varied with sediment elevation and slope, and so a method was needed to specify the location of the image centre. Following Huang et al. (1988), a threshold intensity was used to find the width of the image on the array, and the centre of the image was assumed to lie midway between the first and second threshold crossing. The image position is referred to as the scan count.

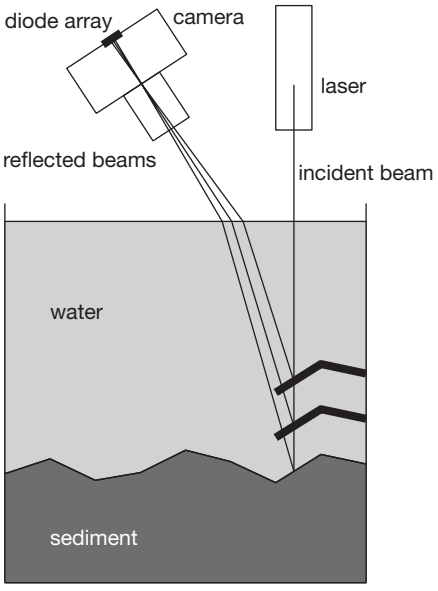

Fig. 1. Positions of laser and camera relative to the sediment surface. Three possible sediment heights are illustrated to demonstrate the change in image location on the photodiode array. Diagram is not to scale

Huang et al. (1988) provided analytical equations to determine elevation from the scan count, assuming that the absolute positions of the camera and laser are known. In practice, the geometry of the camera and laser arrangement cannot be determined to the accuracy required, and higher accuracy is obtained by calibrating image positions against a surface of known geometry. In these experiments, the camera was in the air, while the sediment was under water. Direct calibration before and after each scan avoids complications due to refraction at the water surface.

Four aquaria, each 37 cm × 57 cm, were positioned beneath the traversing frame and filled with sediment sourced from Corunna Lake, an estuary near Narooma, New South Wales, in south-eastern Australia. This lake has a narrow opening to the ocean, and, at the time of sampling, the intertidal sand flats were inhabited by dense populations of thalassinidean shrimp (mainly *Trypaea australiensis*). The sediment and the animals used in the experiments were taken from these tidal flats. Artificial seawater was continuously circulated through a combined pump and filtration system for the duration of the experimental period. The sediment depth was between 25 and 27 cm and the water depth was between 7 and 9 cm in each aquarium. An air conditioner maintained the room at approximately 20°C.

Three of the aquaria contained 3 adult *Trypaea australiensis* individuals each, while the fourth aquarium was left without animals. Animal lengths (measured from eyes to anterior end of telson) ranged from 35.7 to 42.6 mm. Each populated aquarium contained 1 male and 2 females. The animals were constrained to build their burrows in the centre of each aquarium (a 30 cm × 40 cm area) by the insertion of solid aluminium 'fences' that extended to the base of each aquarium. The fences were needed so that the animals would not burrow near the calibration ramps. Further, measurements could not be made at the edges of the aquaria (aquarium walls blocked the camera's line of sight), so it was more convenient to ensure that the animals were burrowing well away from the walls. The diet of these animals is unknown, but frozen zooplankton was added to the water regularly to ensure fresh organic matter would make its way into the animals' burrows.

Each aquarium scan comprised 161 lines. The lines were spaced at 2 mm apart (the resolution in the *x*-direction), were 420 mm long (*y* direction), and the spatial resolution in the *y*-direction was 1 mm. The detection resolution was actually much finer than 1 mm in the *y*-direction, as the scanner detected an average of 18 points over each millimetre section (standard deviation under 4 points). Only the average scan count over each 1 mm section and the number of points forming this average were saved, so 1 scan produced 2 matrices each containing 161 × 420 elements. Scanning time for each aquarium was 1.5 h, so at least 6 h were needed to scan all 4 aquaria.

Scans were usually separated by approximately 2 wk, but there were periods of more frequent scanning on Aquarium 1. The shrimp were introduced to the aquaria on Day 1. The sediment surface was cleared of all mounds by levelling the surface on Day 111 so that recovery from surface disturbance could be observed. Analysis was divided into 2 time periods. Time Period 1 is Day 1 to 110, and Time Period 2 is Day 111 to 359.

Data analysis. All data analysis was conducted in Matlab™. Analysis comprised calibration, map construction and individual mound analysis, as described in the following 3 sections.

Calibration: Before each aquarium scan, the camera focus was altered to get the sharpest signal on the CRO. Calibration was required prior to each scan, and a post-scan calibration was conducted so that an estimate of any calibration drift over the experiment could be obtained.

A calibration ramp was mounted on the inside of one of the walls of each aquarium. The ramp was a solid length of plastic, 150 mm in length and 20 mm wide, positioned at an angle to the sediment surface (elevation changing along a scan line); the upper end of each ramp extended out of the water, and the lowest end extended below the sediment surface level.

The ramp elevation was measured relative to the top of each aquarium. Ramp elevation was measured at

5 or 6 points for each ramp, and linear relationships were found to describe ramp elevation (z) as a function of horizontal location y ($R^2 > 0.9995$). The elevations along the calibration ramps were measured either 2 or 3 times during the first 2 wk of experiments, and again at the end of all experiments just under a year later. Measured values within the first 2 wk differed by at most 0.5 mm, and, after a year, the ramp locations had changed by at most 1.5 mm and were more typically under 0.5 mm from original measurements.

Calibration involved traversing the camera and laser over the length of the calibration ramp so that the image position on the diode array was known over the height range of interest. At the beginning and end of each aquarium scan, the calibration ramps were scanned 5 times, producing scan count values for known y locations. There were 53 scans of Aquarium 1 and 33 of the other 3 aquaria, with each scan yielding 10 calibration scans. The values across the 10 scans were averaged, the elevations at these locations were calculated from the linear relationship described above, and a third-order polynomial fit was found relating elevation (z) to scan count (c). Note that a linear relationship would be adequate to describe elevation as a function of scan count, but a third-order polynomial captured slight curvature in the relationship and allowed an improved fit. A sample calibration curve is shown in Fig. 2. There were 152 calibration polynomials (one for each scan) produced using this technique. Residuals were calculated by taking the absolute value of the difference between ramp elevations and elevations calculated from the third-order polynomial. The mean residual was 0.18 mm (standard deviation = 0.17 mm), and the maximum residual was 1.09 mm.

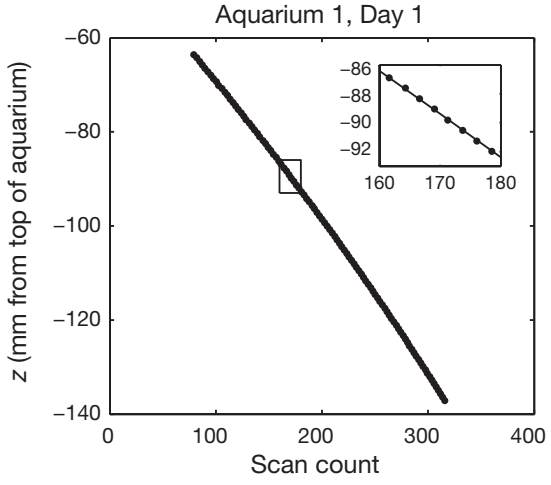

Fig. 2. Sample calibration curve showing calibration scans and fitted polynomial. The inset shows the section marked in the box

Map construction: Raw scan count matrices were converted to elevation using the calibration polynomials. The resulting elevation matrices are readily viewed as 3-dimensional maps and animation sequences. Example surface maps for Aquarium 1 are shown in Fig. 3. The shadows in the images (due to a simulated light source) are to assist 3-dimensional mound visualisation. All mound maps and a movie sequence of mound topography are available in the electronic supplementary material (www.int-res.com/articles/suppl/m329p157_apps/).

Individual mound analysis: Although 3 individuals were added to each aquarium, it could not be established how many animals were alive throughout the experiment. In the field, mounds can be identified easily, but the relationship between the number of mounds and the number of individuals is highly variable (McPhee & Skilleter 2002). For these reasons, volumes and rates of change of volumes were calculated for each mound without attempting to assign them to individual animals.

Mound regions were identified by tagging locations that experienced elevation changes of >15 mm over the measurement period of interest (i.e. any locations whose maximum and minimum elevation over this period dif-

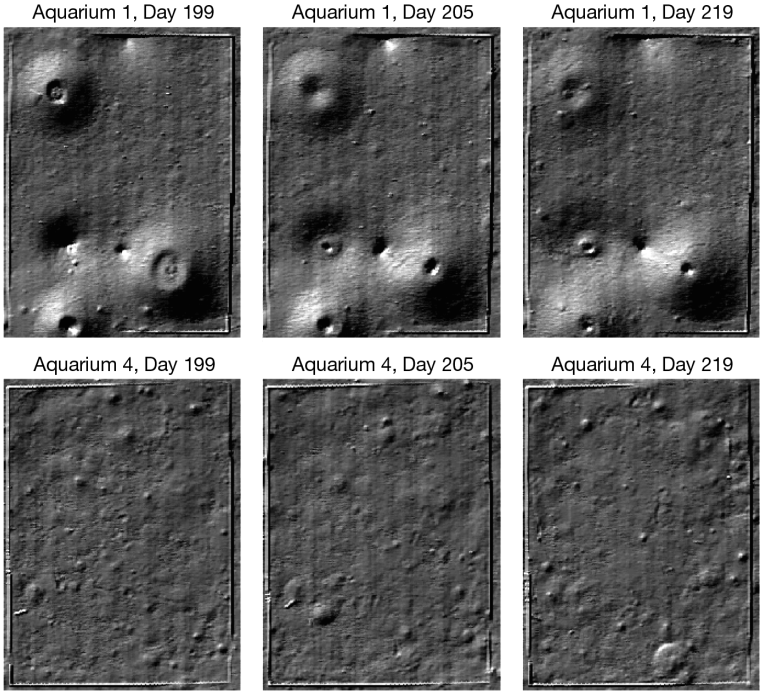

Fig. 3. Examples of elevation maps from Aquarium 1 and the control Aquarium 4, Time Period 2. Colour maps with a scale indicating elevations for all aquaria are available in the electronic supplementary material

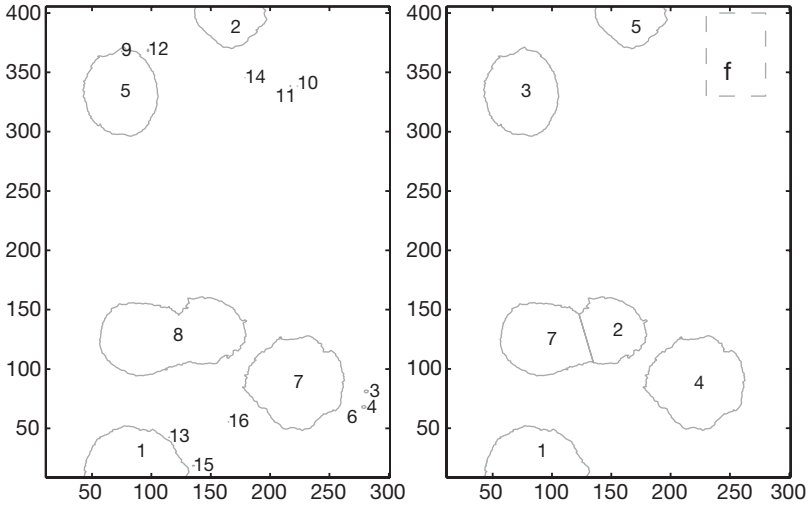

Fig. 4. Example of mound region detection (Aquarium 1, Time Period 2). The left panel shows the raw mound regions identified by 15 mm contour lines as described in the text, and the right panel shows the final mound regions after manual editing. Manual editing included: polygons have been closed (e.g. lower edge has been added to Mound 1), and mound regions have been split (e.g. compare Mound 8 [left] and Mounds 2 and 7 [right]). Small regions, not obviously associated with a mound, have been removed (e.g. Mound 3 [left]). Axis dimensions are given in mm. The rectangular region marked 'f' is the non-mound area referred to in calculations for Fig. 9

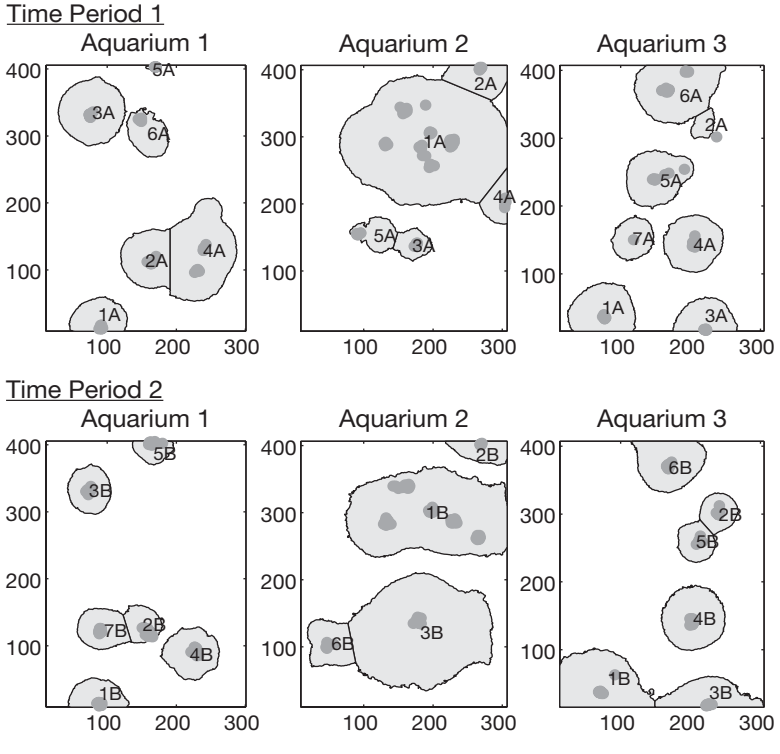

Fig. 5. Mound regions for Aquaria 1 to 3 for both time periods. Mound regions encompass any location that experienced elevation changes of >15 mm over the entire measurement period of interest, and so represent a maximum possible extent of each mound. Dark grey circles mark all hole locations that existed during the lifetime of each mound (Time Period 1: Days 1 to 110; Time Period 2: Days 111 to 359). Axis dimensions are given in mm

fered by >15 mm were tagged). The 15 mm contour lines were then edited manually to close polygons and to split some regions into separate mounds, where possible (Fig. 4). All mound regions were defined to lie within the 'fenced' area. Volume changes were calculated within the mound regions using trapezoid numerical integration. Some mounds spilled material over the fence, and so volume estimates for these mounds are an underestimate.

Once mound regions had been identified for each time period, burrow openings were manually located for each scan. All mounds and their openings for each time period are shown in Fig. 5. The diagrams show only the area that was enclosed by the fence. The mound area and average (mode) number of openings for all mounds are given in Table 1.

RESULTS AND DISCUSSION

Qualitative observations

The sediment was not sieved prior to filling the aquaria. The sediment was sorted by hand to remove any obvious macrofauna (mainly molluscs), but small worms and other meiofauna remained. Their presence explains the changes in sediment surface observed in Aquarium 4 (Fig. 3), and away from mound regions in the other aquaria. The openings to the *Trypaea australiensis* burrows are unmistakable, and are easy to distinguish from the smaller surface changes caused by other organisms.

Burrow openings, once formed, tended to remain in place in undisturbed conditions. Even after clearing the surface on Day 111, the general position of the burrow openings remained largely unchanged.

Individual mounds were observed in Aquaria 1 and 3; however, Aquarium 2 was quite different. Many burrow openings were concentrated into a relatively small area, creating a 'giant' mound comprising many holes (Mound 1, Aquarium 2; Fig. 5). Further, the holes in this mound were less permanent.

Burrow openings were observed to open and close on a daily basis. Some mounds were observed to collapse and change into funnels over time (e.g. mound cross-sections in Fig. 6). It is clear from such exam-

Table 1. Area and average (mode) number of openings for each mound. The mounds and openings are illustrated in Fig. 5

Mound region	— Aquarium 1 — No. of openings (mode)	Area (cm^2)	— Aquarium 2 — No. of openings (mode)	Area (cm^2)	— Aquarium 3 — No. of openings (mode)	Area (cm^2)
Time Period 1						
1	1	33.96	4	360.01	1	56.66
2	1	53.64	1	34.43	1	11.26
3	1	73.91	1	18.37	1	34.4
4	1	111.57	1	20.07	1	55.27
5	1	0.82	1	23.22	1	59.42
6	1	31.03	–	–	1	85.58
7	–	–	–	–	1	28.67
Time Period 2						
1	1	28.85	5	255.23	1	90.24
2	1	23.27	1	23.2	1	24.16
3	1	35.3	1	268.46	1	45.01
4	1	47.66	1	0	1	67.34
5	1	15.53	1	0	1	24.96
6	1	0	1	39.52	1	61.05
7	1	36.63	–	–	–	–

ples that downward transport of sediment surface into burrows can be significant, and, on occasion, more material must have collapsed into the opening than was originally expelled from it. Some openings never formed a mound, and so were sites of downward transport only. Where a mound and a funnel were close to one another, mound material was observed to move down into the neighbouring funnel.

It is clear from the scan data that the burrow openings are sites of relatively rapid 2-way exchange of solid material between the surface and depth. The scan data are used to calculate rates of transport associated with these surface changes.

The locations of burrow openings were largely unaffected by the surface clearing on Day 111 (compare Time Periods 1 and 2 in Fig. 5).

Volume estimates

The difference in the elevation maps from one scan to the next was used to calculate changes in volume over time. Volumes were computed using trapezoidal numerical integration over mound areas. Between any 2 scans, elevation rose at some coordinates and fell at other locations within a particular mound region. Consequently, simply integrating the changes in elevation over a mound region may yield a net volume change that is close to zero, where in fact there has been significant sediment transport in both directions. For this reason we kept upward and downward transport separate when calculating integrals, so that for each mound region we know the total volume rise and volume fall between 2 scans. We also calculated the net volume change, derived from the sum of the rise and fall volumes. An example is given in Fig. 7.

Fig. 8 shows an example of the cumulative volume rise, fall and net change over time for a mound region (Mound 4, Aquarium 1) in each time period. The data from Day 359 have been excluded; 77 d elapsed

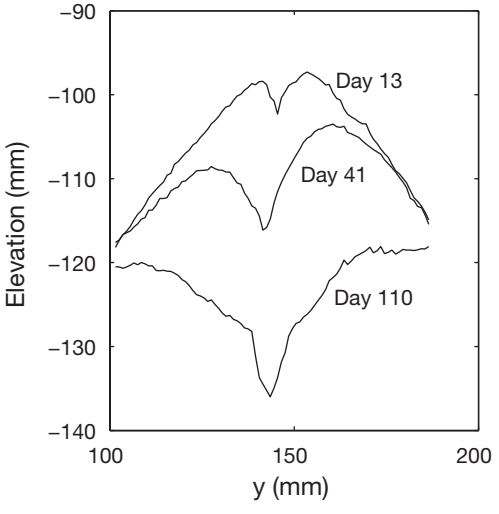

Fig. 6. Example of a mound changing into a funnel. Cross-section in the y direction of Mound 4A in Aquarium 3. Elevation in mm is measured relative to the aquarium top

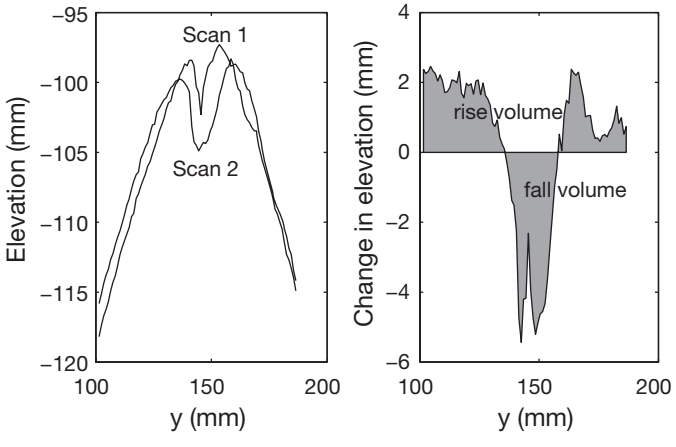

Fig. 7. Example of the elevation changes between 2 consecutive scans, 14 d apart (left panel), and the associated rise and fall volumes (right panel)

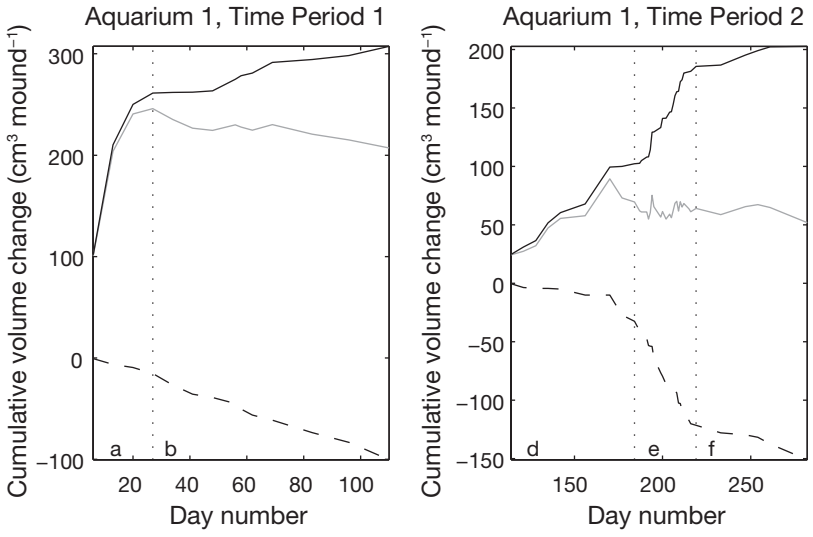

Fig. 8. Cumulative volume changes for Mound 4, Aquarium 1. Dark solid lines show cumulative volume rise, dark dashed lines show cumulative volume fall and grey solid lines show cumulative net volume change. Time Period 1 has been split into a start-up Period a (3 wk) and a subsequent Period b. Cumulative volumes were reset to zero at the end of the start-up period and at the end of Time Period 1; resetting to zero allows easier comparison between the 3 periods. Dotted lines marking Section e in Time Period 2 show the period of higher-frequency sampling for Aquarium 1. The slopes in the cumulative volume rise and fall lines are markedly steeper over this period

between the second last and last scan (Days 282 and 359), whereas the usual interval between scans had not been longer than 3 wk.

Time Period 1 has been split into a 'start-up' Period a and subsequent Period b. The start up period (Day 1 to 27) captures the large volume expulsion during initial burrow construction. Following this initial burrow construction, volume changes are most likely due to routine burrow maintenance, feeding and burrow extension. Forster & Graf (1995) reported that *Callianassa subterranea* specimens were observed to extend their burrows continuously for periods of over a year. Stamhuis et al. (1996) measured behaviour and time allocation of *C. subterranea* in laboratory aquaria and found that 27% of the animals' time was spent burrowing (defined as any interaction with the sediment and transport activities — stirring, lifting, carrying, dropping, tamping, bulldozing, pumping — and would include feeding). Stamhuis et al. (1997) measured the total length of *C. subterranea* tunnel systems over time, and found that initial burrowing velocity (increase in total burrow length per hour) was much higher for approximately the first 4 d of new burrow construction. Rates of volume change in our experiments, inferred from weekly sampling for the first 10 wk, suggested that an initial period of high expulsion rates lasted for a period of approximately 3 wk. The period of high expulsion was estimated from the change in slope in the cumulative volume rise graphs, e.g. Fig. 7.

Total rates of volume rise and fall and the net volume change for the mound regions in each aquarium are given in Table 2. These rates were calculated by dividing the final cumulative volume changes (summed across all mounds) by the number of days elapsed. Start-up rates of volume rise were much higher in the start-up period, and exceeded rates in subsequent periods by a factor of 3.4 to 9.7. In this period there is a clear net delivery of sediment to the surface at rates ranging from 18.9 to 22.9 $cm^3\ d^{-1}$. In subsequent periods net delivery to the surface is much lower, and can even be negative (a range of −1.3 to 6.2 $cm^3\ d^{-1}$). The relatively low rates of net delivery, however, are the result of higher rates of transport in both directions; in Time Periods 1b and 2 the rates of volume rise and fall are comparable to one another and range from 2.6 to 9.1 $cm^3\ d^{-1}$ (rise) and 2.9 to 6.9 $cm^3\ d^{-1}$ (fall). These measurements question the assumption underlying direct trapping techniques that the mounds are primarily a source of material from depth.

Mean rates of volume rise, fall and net change were calculated by dividing the final cumulative volume changes for each mound (rise, fall and net) by the number of days elapsed, and taking the mean of all mounds. There was usually only 1 opening associated with a mound region; however, Mound 1 in Aquarium 2 typically had 4 or 5 openings (Table 1). The rate of volume change for this mound region far exceeded that of the other mound regions. Rather than have this mound bias the mean rate per mound, and given that

Table 2. Total rate of volume rise, fall and net volume change ($cm^3\ d^{-1}$) within mound areas

Aquarium	Volume rise	Volume fall	Net volume change
Time Period 1a (start-up)			
1	25.23	−2.31	22.92
2	31.36	−2.45	28.91
3	20.88	−2.02	18.87
Time Period 1b			
1	2.61	−3.86	−1.25
2	9.11	−2.9	6.21
3	4.76	−4.35	0.41
Time Period 2 (excluding Day 359)			
1	3.91	−3.59	0.32
2	7.17	−6.93	0.24
3	4.42	−3.4	1.02

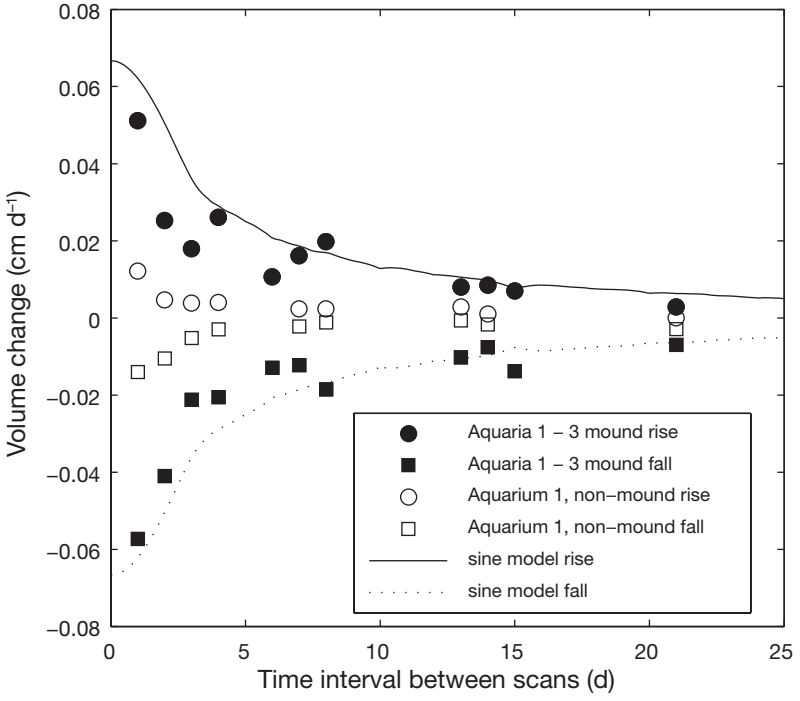

Fig. 9. Mean rate of volume change per unit area between scans. Solid symbols indicate data from mound regions, and open symbols indicate data from the non-mound Region 'f' indicated in Fig. 4. The theoretical curves from assuming a generic Fourier series (Eq. A5) are marked, and have been calculated using Eq. (A6). Values of a_n were set to $1/(10n)$ if $n < 10$, and zero otherwise, and T was set to 15

the openings are the source or sink of the sediment, rates were normalised by the mode number of openings for each mound. Rates are quoted in units of cubic centimetres per day per opening, and the mean rates and standard deviations of volume rise, volume fall and net volume change per opening for 3 time periods (start-up period, remainder of Time Period 1 and Time Period 2) are given in Table 3.

Sampling frequency effects

Strong sampling frequency dependence is apparent in the data. Aquarium 1 was scanned more frequently than the other aquaria between Days 184 and 219 (Time Period 2), and the cumulative volume rise and fall graphs were markedly steeper between these days when compared with previous and subsequent days (see Fig. 8, Time Period 2, Section e). To investigate this effect further we calculated the mean rate of volume change per unit area between scans in all mound regions, and plotted them against the time interval between scans (Fig. 9). Rates of volume change clearly increase with decreasing time interval. The same effect is seen in a 'flat' region away from the mounds (marked as Region f in Fig. 4), suggesting that the activity of the smaller animals in the tank produces a similar pattern at a smaller scale.

This pattern is consistent with sampling an oscillating signal. We investigated this effect by simulating an oscillating sediment surface using equations described in Appendix 1. An example of a theoretical curve from these equations is given in Fig. 9, and it captures the behaviour observed in the data. Note that the problem is not simply an aliasing issue, which could be remedied by ensuring that the Nyquist frequency of the measured time series is high enough. Given an oscillating signal containing a maximum frequency f_{max}, a sampling frequency of $f_s \geq 2f_{max}$ is required to detect f_{max} in the measured time series and avoid aliasing errors (Nyquist 2002). In the example given in Fig. 9, the period of oscillations is 30 d, yet sampling every 15 d is inadequate to estimate the rate of volume change. Nyquist's result is about capturing the correct frequency information from data; however, in our case, we not only want to estimate the frequency of oscillations accurately, but to integrate the time series to estimate cumulative volumes. The accuracy of this estimation will continue to improve with sampling frequencies $>2f_{max}$.

The impact of sampling interval on rates of volume change is substantial. Fig. 10 shows the same scan data sampled at different frequencies (Aquarium 1, Day 184 to 219). During this period of time, Aquarium 1 was sampled more frequently than the other aquaria (typically daily, with some exceptions). The other aquaria

Table 3. Mean rates of volume rise, volume fall and net volume change per opening for each aquarium and each time period ($cm^3\ d^{-1}$ burrow opening^{-1})

Aquarium	Volume rise (SD)	Volume fall (SD)	Volume change (SD)
Time Period 1a (start-up)			
1	4.2 (3.81)	−0.38 (0.34)	3.82 (3.63)
2	2.05 (2.84)	−0.24 (0.18)	1.8 (2.74)
3	2.98 (1.82)	−0.29 (0.18)	2.7 (1.7)
Time Period 1b			
1	0.64 (0.59)	−0.66 (0.47)	−0.02 (0.5)
2	0.81 (0.93)	−0.32 (0.17)	0.48 (0.91)
3	0.92 (1.15)	−0.65 (0.48)	0.27 (1.17)
Time Period 2 (excluding Day 359)			
1	0.52 (0.42)	−0.47 (0.28)	0.04 (0.26)
2	0.36 (0.38)	−0.82 (1.52)	−0.47 (1.46)
3	0.68 (0.52)	−0.53 (0.33)	0.15 (0.67)

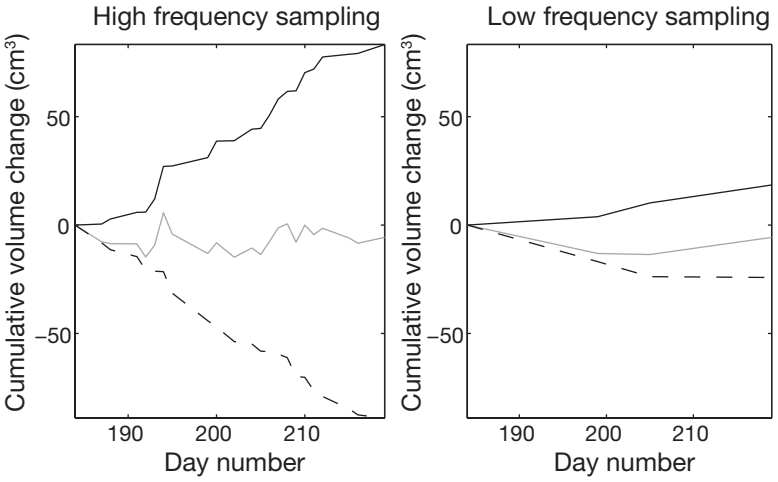

Fig. 10. Cumulative volume changes for Mound 4, Aquarium 1, Days 184 to 219, sampled at different frequencies. Left panel: all data were used; right panel: the data were sampled less frequently (at the same frequency as the other aquaria). Dark solid lines show cumulative volume rise, dark dashed lines show cumulative volume fall and grey solid lines show cumulative net volume change

were only sampled on Days 184, 199, 205 and 219. The rates of volume change from these 2 scenarios are given in Table 4. The calculated rates are 3 or 4 times higher than those calculated from the same data subsampled on Days 184, 199, 205 and 219. (The rates of net volume change remain the same as this is determined only by the first and last scan of the sampling period.) The essential point is that the sampling rate has a major effect on our ability to estimate instantaneous rates of volume change.

It is apparent from the maps constructed from the frequent scans of Aquarium 1 (available as electronic supplementary material at www.int-res.com/articles/suppl/m329p157_apps/) that the mound holes open and close on a daily basis, creating an oscillating change in elevation near the opening of each mound. The results in Table 4 demonstrate that if this oscillation is sampled less frequently than daily, much of the upward and downward transport is missed and calculated rates of volume rise and fall are underestimates. We cannot rule out the possibility that even daily measurements are insufficient to adequately characterise the oscillatory sediment transport. A spectral analysis of higher-frequency measurements would be needed to draw more definitive conclusions about adequate sampling frequencies.

Table 4. Influence of sampling frequency on calculated mean rates of volume change ($cm^3\ d^{-1}$ opening^{-1})

	Volume rise (SD)	Volume fall (SD)	Volume change (SD)
Frequent sampling	1.15 (0.87)	−1.3 (0.93)	−0.15 (0.43)
Infrequent sampling	0.29 (0.26)	−0.44 (0.38)	−0.15 (0.43)

Comparison with published studies

The laboratory conditions were ideal for demonstrating the need for high temporal and spatial resolution mound measurements; however, they were not suitable for accurately estimating *Trypaea australiensis* sediment turnover rates. The animals were housed in very shallow aquaria, with artificial diet and seawater, none of the usual daily and seasonal variations in their environment and no interactions with other macrofauna. Nevertheless, comparisons with published estimates from this and other thalassinidean shrimp are warranted.

In these experiments, volumetric sediment transport was measured rather than mass. Mean rates of sediment rise ranged from 0.36 to 1.1 $cm^3\ d^{-1}$ opening^{-1}, and mean rates of sediment fall ranged from −0.32 to −1.3 $cm^3\ d^{-1}$ opening^{-1} (Tables 3 & 4, excluding start-up period). If a porosity of 0.4 and a sand density of 2.65 g cm^{-3} are assumed, these rates correspond to a range in sediment rise rates from 210 to 670 g opening^{-1} yr^{-1} and a range of sediment fall rates from 190 to 750 g opening^{-1} yr^{-1}. The population density of *Trypaea australiensis* varies widely. Further, measurements by McPhee & Skilleter (2002) demonstrate that inferring animal density from mound opening density can be done only poorly, so, without actively digging up the field site, the actual numbers of animals residing in an area cannot be determined and only mound openings can be counted reliably. Based on our laboratory measurements, assuming 20 burrow openings m^{-2} and the lower expulsion rate, rates of sediment rise could be as low as 4.2 kg m^{-2} yr^{-1}. If there are 200 burrow openings m^{-2} and the higher expulsion rate, rates of sediment rise could be as high as 134 kg m^{-2} yr^{-1}. The densities at the field sampling site, Corunna Lake, were not measured accurately, but lie at the lower end of this range. Rates of sediment fall would cover a similar range.

There are good reasons for believing that higher volume rates would be inferred if these experiments were to be repeated in the field. Comparisons between field and laboratory measurements for other species of thalassinidean shrimp have revealed large differences. The following examples all used direct entrapment measurement techniques.

Bird (1997) estimated sediment turnover rates for *Biffarius arenosus* in the field and found ejection rates of 4.26 g dry mass sediment ind.$^{-1}$ d^{-1} (population density of 8.7 shrimps m^{-2}). Her earlier measurements conducted in the laboratory (using the same species) had produced a sediment turnover estimate of 0.79 g dry mass ind.$^{-1}$ d^{-1} (Bird et al. 1997).

Laboratory-derived estimates for *Callianassa subterranea* are 15 kg m^{-2} yr^{-1} (Stamhuis et al. 1997) and 11 kg m^{-2} yr^{-1} (Rowden et al. 1998), yet the same methods used in the field for *Callianassa filholi* yielded a sediment turnover rate of 96 kg m^{-2} yr^{-1} (Berkenbusch & Rowden 1999), even though the density of *C. subterranea* individuals was 2.5 times higher than the density of *C. filholi* (11 to 25 ind. m^{-2}, or 7.5 to 19.2 mounds m^{-2} measured for *C. filholi*) and the animals are deposit feeders of a similar size.

Berkenbusch & Rowden (1999) suggested that the large difference between the 2 measurements reflects the fact that the *Callianassa subterranea* measurements were made under constant laboratory conditions, while the *Callianassa filholi* measurements were made *in situ* and accounted for a number of physical factors (including temperature variation, animal size and burrow position relative to the shore). Other burrowing animals in the field would encounter and damage thalassinidean burrows, so creating more burrow maintenance work for the inhabitants. Other contributing factors to differences between field and laboratory measurements could be the presence of juveniles and post-larval shrimp in field studies (they were absent from the laboratory studies), and the fact that the *C. filholi* measurements were made on an intertidal sandflat (the authors believe there may be a significant difference in sediment turnover rates between intertidal and subtidal populations). Berkenbusch & Rowden (1999) noted strong seasonal variation in *C. filholi* sediment turnover rates (higher rates in spring and summer). There has been speculation that thalassinidean sediment turnover rates are influenced by sediment nutrient content; however, measurements reported by Stamhuis et al. (1997) were unable to confirm a significant effect.

Feasibility of field measurements

The animals in our experiments were housed in laboratory aquaria that were free from the disturbances typically experienced in the field. In principle, similar experiments could be repeated in a field setting. The non-destructive nature of the method and the high spatial resolution would yield more accurate measurements than direct entrapment techniques.

Three main challenges of repeating such an experiment in the field include: (1) protecting electronic equipment and the metal traversing frame from saltwater conditions; (2) ensuring a smooth water surface during the scanning period, perhaps by floating a Perspex sheet on the surface; and (3) the scan time may be a limiting factor. For all of these reasons stereo-photogrammetry may be a more feasible technique for producing high-resolution elevation maps. Photogrammetry has the additional advantage of allowing maps to be constructed in deeper water. Bythell et al. (2001) successfully employed underwater photogrammetry to characterise morphological characteristics of coral accurately. The important point is that high-frequency, high-resolution maps of the sediment surface allow a more complete picture of sediment turnover to be assessed; the measurements need not be made by a laser scanner.

Relevance to sediment biogeochemistry

We surmise from these experiments that efforts to characterise sediment mixing with a single 'sediment turnover rate' may be misguided. These experiments suggested there are highly localised sites of exchange between sediment and depth, surrounded by relatively quiescent regions. The biogeochemistry of sediments structured in this way is likely to differ widely from sediment mixed uniformly according to a single sediment turnover rate, as there may be 'hotspots' of organic material and oxygen supply fed by the mound openings (e.g. Harper et al. 1999). Diagenetic processes are sensitive to the sediment transport environment. Conveyor-belt mixing, diffusive mixing and burrow-and-fill mixing are all capable of producing similar profiles for radionuclide tracers (Boudreau 1986a,b, Boudreau & Imboden 1987), yet can have different effects on diagenesis reaction pathways. Aller (1994) demonstrated that oscillating conditions lead to quite different diagenetic consequences than do static conditions. An area containing a small volume of sediment that oscillates daily between the surface and depth, while surrounded by comparatively static sediment, is likely to process organic matter very differently compared to a sediment area that is uniformly mixed at the same spatially averaged rate (i.e. all sediment being mixed, but at a much lower rate).

Knowledge of how organic matter and other materials are mixed in sediments is essential if we are to better understand these interactions with sediment biogeochemistry. In particular, time and length scales of transport processes can be incorporated into non-local transport–reaction models of sediment diagenesis

(Boudreau 1986b, Boudreau & Imboden 1987, Choi et al. 2002). Our experiments have demonstrated that high-frequency, high-resolution maps of the sediment surface may reveal a more subtle picture of these transport processes than can be gleaned from direct entrapment or tracer methods. The dynamic information inferred from these experiments has also been used to inform subsequent bioturbation modelling (Grigg 2003). Similar mapping exercises could be undertaken for other bioturbating animals to assess the difference between net and gross sediment transport at the sediment surface. Such mapping is useful for characterising the time scales of mixing, but the depths to which surface material is translocated remains unknown. Assessing the distribution of sediment turnover times and depths within the sediment is a significant challenge and will not be resolved using any present techniques.

CONCLUSION

These experiments demonstrated the effectiveness of adopting a non-destructive, high-resolution and high-frequency approach to measuring sediment turnover. The experiments yielded useful insights into the creatures' burrowing habits and raised important methodological considerations. Our 2 main conclusions are: (1) burrow openings function as conduits of rapid 2-way exchange between the sediment surface and depth; slumping and mound formation both occur simultaneously and are a surface reflection of subterranean processes; (2) the oscillatory nature of sediment transport at mound openings creates the potential for aliasing errors in measuring transport rates unless a high sampling frequency is employed. The net rate is independent of sampling interval, but we have demonstrated that this net rate masks a much higher gross rate of sediment transport. The results suggested that laboratory aquaria should be scanned daily or more frequently to avoid such errors.

Neglecting these 2 important points potentially leads to significant underestimation of thalassinidean shrimp sediment turnover estimates. Further, it is not clear whether sediment trapping techniques capture the net rate, especially if the trap alters the way material slumps back into the burrow. Other studies have demonstrated the importance of additional effects when interpreting sediment turnover measurements. These effects include temperature, population density, body size and tidal patterns (Stamhuis et al. 1997, Rowden et al. 1998, Berkenbusch & Rowden 1999). We suggest that impacts of oscillatory processes also be considered when interpreting sediment transport measurements.

Acknowledgements. The laser scanner was constructed by J. Taylor in the Pye Laboratory, CSIRO, in the early 1990s. We thank D. E. Hughes and G. Miller for their substantial assistance in re-assembling the laser scanner. These experiments were conducted as part of N.J.G.'s PhD research at CSIRO Land and Water and the Centre for Resource and Environmental Studies, Australian National University (ANU), funded by a Commonwealth Government Australian Postgraduate Award and the Water Research Foundation. Her supervisor at ANU was I. White. We thank B. S. Sherman, F. L. Bird and 4 anonymous reviewers for their careful reviews and helpful suggestions.

LITERATURE CITED

Aller RC (1994) Bioturbation and remineralization of sedimentary organic matter — Effects of redox oscillation. Chem Geol 114:331–345

Berkenbusch K, Rowden AA (1999) Factors influencing sediment turnover by the burrowing ghost shrimp *Callianassa filholi* (Decapoda: Thalassinidea). J Exp Mar Biol Ecol 238: 283–292

Bird FL (1997) Burrowing and feeding ecology of the ghost shrimp *Biffarius arenosus* (Decapoda: Callianassidae). PhD dissertation, Victoria University of Technology, Melbourne

Bird FL, Ford P, Heislers S (1997) Bioturbation by common Port Phillip Bay benthic invertebrates. Technical Report No. 37, Port Phillip Bay Environmental Study, CSIRO Environmental Projects Office, Canberra

Bird FL, Ford PW, Hancock GJ (1999) Effect of burrowing macrobenthos on the flux of dissolved substances across the water–sediment interface. J Mar Freshw Res 50:523–532

Boudreau BP (1986a) Mathematics of tracer mixing in sediments. I. Spatially dependent, diffusive mixing. Am J Sci 286:161–198

Boudreau BP (1986b) Mathematics of tracer mixing in sediments. II. Nonlocal mixing and biological conveyor-belt phenomena. Am J Sci 286:199–238

Boudreau BP, Imboden DM (1987) Mathematics of tracer mixing in sediments. III. The theory of nonlocal mixing in sediments. Am J Sci 187:693–719

Bythell JC, Pan P, Lee J (2001) Three-dimensional morphometric measurements of reef corals using underwater photogrammetry techniques. Coral Reefs 20:193–199

Choi J, Francois-Carcaillet F, Boudreau BP (2002) Lattice-automaton bioturbation simulator (LABS): implementation for small deposit feeders. Comput Geosci 28:213–222

Dworschak PC (2000) Global diversity in the Thalassinidea (Decapoda). J Crustac Biol 20:238–245

Forster S, Graf G (1995) Impact of irrigation on oxygen flux into the sediment: intermittent pumping by *Callianassa subterranea* and "piston-pumping" by *Lanice conchilega*. Mar Biol 123:335–345

Grigg NJ (2003) Benthic bulldozers and pumps: laboratory and modelling studies of bioturbation and bioirrigation. PhD dissertation. Australian National University, Canberra. Available at http://thesis.anu.edu.au/public/adt-ANU20060228.104425/index.html

Harper MP, Davison W, Tych W (1999) One-dimensional views of three-dimensional sediments. Environ Sci Technol 33: 2611–2616

Huang C, White I, Thwaite EG, Bendeli A (1988) A noncontact laser system for measuring soil surface topography. Soil Sci Soc Am J 52:350–355

McPhee DP, Skilleter GA (2002) Aspects of the biology of the yabby *Trypea australiensis* (Dana) (Decapoda : Thalassinidea) and the potential of burrow counts as an indirect

measure of population density. Hydrobiologia 485:133–141
Nyquist H (2002) Certain topics in telegraph transmission theory (reprinted from transactions of the A.I.E.E., February 1928, p 617–644). Proc IEEE 90:280–305
Rowden AA, Jones MB (1993) Critical evaluation of sediment turnover estimates for Callianassidae (Decapoda: Thalassinidea). J Exp Mar Biol Ecol 173:265–272
Rowden AA, Jones MB, Morris AW (1998) The role of *Callianassa subterranea* (Montagu) (Thalassinidea) in sediment resuspension in the North Sea. Cont Shelf Res 18: 1365–1380
Stamhuis EJ, Reede-Dekker T, van EY, de WJJ, Videler JJ (1996) Behaviour and time allocation of the burrowing shrimp *Callianassa subterranea* (Decapoda, Thalassinidea). J Exp Mar Biol Ecol 204:225–239
Stamhuis EJ, Schreurs CE, Videler JJ (1997) Burrow architecture and turbative activity of the thalassinid shrimp *Callianassa subterranea* from the central North Sea. Mar Ecol Prog Ser 151:155–163
Webb AP, Eyre BD (2004) Effect of natural populations of burrowing thalassinidean shrimp on sediment irrigation, benthic metabolism, nutrient fluxes and denitrification. Mar Ecol Prog Ser 268:205–220
Ziebis W, Forster S, Huettel M, Jørgensen BB (1996) Complex burrows of the mud shrimp *Callianassa truncata* and their geochemical impact in the sea bed. Nature 382:619–622

Appendix 1. Equations for simulating oscillating sediment surface

We investigated the effect of sampling an oscillating sediment surface using sine functions. For example, if the surface elevation h were to rise and fall in a sinusoidal pattern according to the following equation:

$$h(t) = A\sin\left(\frac{2\pi}{T}t\right) \quad \text{(A1)}$$

where t is time (d), A is the amplitude (cm) and T is the period of oscillation (d), the time-averaged rate of volume rise per unit area, r_{av}, is:

$$r_{av} = \frac{1}{nT}\int_0^{nT} r(t)\,dt = \frac{1}{2nT}\int_0^{nT}\left|\frac{dh}{dt}\right|dt \quad \text{(A2)}$$

where n is an integer and

$$r(t) = \begin{cases}\frac{dh}{dt} \text{ if } \frac{dh}{dt} > 0\\ 0 \text{ otherwise}\end{cases}$$

The analytical solution to Eq. (A2) is $2A/T$. Similarly, the time-averaged rate of volume fall per unit area is $-2A/T$ cm d^{-1}, and the time-averaged net rate is 0 cm d^{-1} (Fig. A1). Estimating this rate from measurements will introduce sampling artefacts, and the estimates are particularly prone to aliasing effects. Measurements of surface elevation h separated by a constant time period Δ can be used to approximate the rate of elevation change such that:

$$\left.\frac{dh}{dt}\right|_{t+\Delta} \approx \frac{h(t+\Delta) - h(t)}{\Delta} \quad \text{(A3)}$$

Substituting this approximation into Eq. (A2) does not yield the analytical solution, $2A/T$, but an approximation of r_{av}, r_{est}, that is a function of Δ and $\lim_{\Delta\to 0} r_{est} = r_{av}$:

$$\begin{aligned} r_{est} &= \frac{1}{2nT}\int_0^{nT}\left|\frac{dh}{dt}\right|dt \\ &= \frac{1}{2nT}\int_0^{nT}\left|\frac{A\sin\left(\frac{2\pi}{T}(t+\Delta)\right) - A\sin\left(\frac{2\pi}{T}\right)}{\Delta}\right|dt \\ &= \frac{A}{nT\Delta}\left|\sin\left(\frac{\pi\Delta}{T}\right)\right|\int_0^{nT}\left|\cos\left(\frac{\pi}{T}(2t+\Delta)\right)\right|dt \\ &= \frac{\left|2A\sin\left(\frac{\pi\Delta}{T}\right)\right|}{\pi\Delta} \end{aligned} \quad \text{(A4)}$$

With increasing Δ this function drops rapidly away from $2A/T$ and exhibits nodes where the rates of volume rise or fall per unit area are estimated to be zero. These nodes are not observed in the experimental data, most likely because there is no single frequency of oscillating sediment transport, but a range of frequencies superimposed. Indeed, replacing Eq. (A1) with a more generic oscillating function comprising a superposition of sine waves with amplitude coefficients a_n:

$$h(t) = \sum_{n=1}^{\infty} a_n \sin\left(\frac{\pi n}{T}t\right) \quad \text{(A5)}$$

yields an expression for r_{av} that is capable of exhibiting a range of behaviour, all characterised by a fall in estimated rates of volume rise or fall as Δ increases:

$$r_{est} = \frac{2}{\pi\Delta}\sum_{n=1}^{\infty} a_n\left|\sin\left(\frac{\pi n\Delta}{2T}\right)\right| \quad \text{(A6)}$$

The analytical expression for r_{av} is:

$$r_{av} = \frac{1}{T}\sum_{n=1}^{\infty} n a_n \quad \text{(A7)}$$

and again $\lim_{\Delta\to 0} r_{est} = r_{av}$.

An example of a theoretical curve for r_{est} is given in Fig. 9, and it captures the behaviour observed in the data.

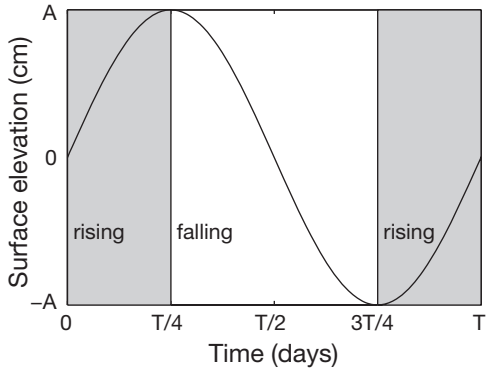

Fig. A1. Surface elevation rising and falling according to Eq. (A1). The sediment surface rises during the first and last quarter, and falls during the middle 2 quarters, as indicated by shading

Editorial responsibility: Otto Kinne (Editor-in-Chief), Oldendorf/Luhe, Germany

Submitted: July 4, 2005; Accepted: May 24, 2006
Proofs received from author(s): December 5, 2006